NRA

National Rivers Authority

Appendix A The Lambourn Catchment Modelling work

A.1 INTRODUCTION

The objective of this part of the study has been to develop a simple numerical model of a typical chalk catchment which could be used for a sensitivity analysis of the impact of groundwater pumping on stream flow with respect to abstraction regimes and aquifer configuration.

The Lambourn catchment is on the Berkshire Downs, which lies on the unconfined Chalk aquifer. This aquifer is the major aquifer in the UK both in areal extent and in the quantity and quality of water extracted from it. The Lambourn catchment was investigated intensively during the 1960s and 1970s for the purposes of the West Berkshire Groundwater Scheme, which had the objective of maintaining downstream river flows during dry periods through augmenting the River Lambourn by groundwater pumping (Hardcastle, 1978).

The Lambourn catchment was chosen for the chalk catchment because of its extensive groundwater and river flow monitoring network developed as part of the West Berkshire Groundwater Scheme. Furthermore, except for short periods when the abstraction scheme was operated, the catchment is relatively natural with only 3 % of the mean flow abstracted for local supply.

The aquifer in the Berkshire Downs has been extensively modelled in the past (Oakes and Pontin, 1976; Connorton and Hanson, 1978; Morel, 1980), and most recently by Rushton *et al.* (1989), who developed a three dimensional model of the complete River Kennet basin for estimating the groundwater resources of the aquifer.

The numerical basis and the assumptions of the model are described. The calibration procedure is discussed, and the calibrated values are compared to values used in other models which have previously been applied to the catchment. Finally, the sensitivity of the catchment low flow response to groundwater abstractions is estimated.

A.2 HYDROGEOLOGY OF THE STUDY AREA

The study area is the 234.1 km^2 catchment of the River Lambourn gauged at Shaw in Newbury (Fig.1). The Lambourn is a tributary of the River Kennet, which drains the Berkshire Downs to the Thames. The only streams within the catchment are the Lambourn itself and the Winterbourne, a northern tributary which joins the Lambourn just upstream of Newbury. The bourne head of the Lambourn varies by up to 7 km downstream from the source shown in Fig. 1. Similarly the bourne head of the Winterbourne varies by about 5 km depending on the groundwater table.

The catchment topography rises from 76 m to 226 m above sea level and has a general slope towards the south east (Fig.1). The irregularly shaped contour lines show the existence of

several dry valleys. The topography and drainage of the region are strongly controlled by geological structure. The region is situated on the northern flank of the London Basin, which is an asymmetrical syncline, dominated by Cretaceous Chalk (Fig. 2). The Chalk has a thickness of more than 200 m and with its northern escarpment forms the catchment boundary with lower ground on the older Greensand and clays to the north. In the central part of the catchment the Chalk is overlain by more impermeable deposits of clay with flint.

The Chalk is a porous, micritic, white limestone divided into a lower, middle and upper zone. Results of geophysical well-logging and pumping tests have shown that groundwater movement is related to fissures mainly parallel to the bedding, and that fissure development is dependent on depth rather on stratigraphy (Owen *et al.*, 1977, Owen and Robinson, 1978). The effective saturated thickness is about 30-50 m.

The transmissivity (T) and storativity (S) vary laterally as well as vertically, the lateral variation having an apparent correlation with topography. Based on four parameters (distance from a main valley, depth to water table, saturated thickness and the proportion of the effective aquifer in the lower Chalk) a hydrogeological model was developed (Owen and Robinson, 1978). According to this model the T value varies horizontally as shown relatively in Fig. 3. The base value for average groundwater levels is $T = 2 \times 10^{-2}\ m^2\ s^{-1}$. The storativity varies in a similar way from 0.4 % to 3 %. In addition to the horizontal variation, the transmissivity decreases with decreasing water levels (Connorton and Reed, 1978) due to a reduction in saturated depth and in the hydraulic conductivity (K).

A.3 NUMERICAL BASIS OF THE ASM MODEL AND REPRESENTATION OF THE AQUIFER PROPERTIES

The ASM model (Aquifer Simulation Model) was applied to the catchment. This is a two-dimensional, finite difference, numerical model, developed by Kinzelbach and Rausch (1989). The model includes a leakage flow term, which is used to simulate the exchange flow between the aquifer and surface water. The program uses the IADI (Iterative-Alternating Direction Implicit) method described by Prickett and Lonnquist (1971) to solve the differential, heterogeneous, isotropic, transient groundwater flow equation:

$$T\left(\frac{d^2\theta}{dx^2} + \frac{d^2\theta}{dy^2}\right) = S\,\frac{d\theta}{dt} + q \qquad (1)$$

where x and y are orthogonal space coordinates, t is time, θ is the water table and q a general flow term including fixed boundary flows, recharge, leakage to/from streams and abstractions. For each iteration T is calculated as K times the saturated depth of the unconfined aquifer. The IADI method is stable for large time steps, which allows monthly data to be used.

A rectilinear mesh was superimposed over the study area such-that the grid lines lie parallel to the major valleys (Fig. 4). The grid size was selected to be 500 m in both directions. The boundary was defined as a non-flux boundary following the groundwater divide determined on the basis of the groundwater potential map marked in Fig. 5. The map is based on mean values of the maximum groundwater level (February-March 1988) and the minimum level

(December 1990) observed during the period 1966-1990 in those wells shown in Fig 5. These mean values are found to be close to the average groundwater levels. The groundwater catchment area was estimated to be 210 km^2, which corresponds to 90% of the topographic catchment area. The bottom of the aquifer in each cell is defined to be 40 m below mean groundwater level. This corresponds to the estimated depth of the major aquifer as published in the literature.

The stream cells, shown in Fig.4, differ from the remainder by including a leakage rate (q_{lea}) between the aquifer and the stream. When the hydraulic head is higher in the aquifer than in the stream the leakage rate is directly proportional to the head difference (θ-h) between that of the aquifer potential head (θ) and the stream surface water level (h), and the hydraulic conductivity of the streambed (p'), and is inversely proportional to the thickness of the streambed material (m'). The constant of proportionality termed the leakage coefficient λ is defined as p'/m'. The leakage rate can thus be calculated as:

$$q_{lea} = \frac{p'}{m'}(\theta - h) = \lambda(\theta - h) \quad . \qquad (2)$$

However, when θ becomes lower than the bottom of the river bed (h_b) the stream cells are represented as a series of tanks draining through the resistance of the streambed. In this case the leakage rate is proportional to the potential head in the stream and can be calculated as:

$$q_{lea} = \lambda(h - h_b) \qquad \text{for } \theta < h_b \quad . \qquad (3)$$

The intermittent nature of the bourne sections of the stream was simulated by defining the stream depth as zero ($h = h_b$) for the stream cells corresponding to the bourne section. Under the condition θ is less than h_b the leakage rate, as defined by equation (3), is zero. Flow routing in the stream cells is achieved by summing cells to the four gauged points in the catchment. While this is sufficient when working on a monthly time step, it does assume the bourne stream cells dry up sequentially from the head waters downstream.

The leakage coefficient is set to 1.0×10^{-7} s^{-1} for all stream cells. This value was estimated from Eq. 2 by inserting simultaneously observed head differences and flow values for each of the four reaches shown in Fig. 4. Both the average situation (mean flow and average groundwater level) and the minimum situation (the Q95, which is the discharge exceeded 95 % of the time, and the minimum groundwater level) were used to estimate the leakage coefficients.

A.4 ESTIMATING GROUNDWATER RECHARGE

The series of monthly streamflows used for the modelling study were the 29 years from 1962 to 1990. During this period four gauging stations were operational (Fig. 1). Their names and the most important flow statistics are given in Table 1. The mean flow (MF) from the catchment at Shaw is 1.72 m^3 s^{-1}, equivalent to 258 mm year^{-1} using the groundwater catchment area.

The mean precipitation (1941-1970) varies from 700 mm year^{-1} in the valleys to 760 mm

year^{-1} on the Downs. The mean recharge to the aquifer was set equal to the recorded mean flow (258 mm year^{-1}). Based on the distribution of rainfall and catchment geology the mean recharge was assumed to be 235 mm year^{-1} in the eastern area and 280 mm year^{-1} in the western area (Fig. 6), where the precipitation is higher and there is no cover of clay with flint.

The seasonal variation of infiltration from the root zone was derived from time series of the effective precipitation for grassland calculated using MORECS (Meteorological Office Rainfall and Evaporation Calculation System). The land use in the Lambourn catchment is dominated by grassland and arable farming, with a limited area of woodland. The root constant for grass is 75 mm, and 100 mm for arable areas. The mean value of the effective precipitation for grassland (1962-1990) calculated from MORECS is 212 mm year^{-1}. This is lower than the value of 258 mm year^{-1} calculated from long term gauged flow records at Shaw. The mean effective precipitation calculated from flow records was used for the study as it was deemed to be more representative of the catchment than the MORECS estimate. The MORECS monthly values were used to temporally distribute the gauged value of mean effective precipitation.

The Base Flow Index (Gustard *et al.*, 1992) is very high at all four gauging stations (Table 1) indicating that rapid response runoff is very limited, a feature which is supported by Morel (1980). This is represented in the model by assuming that all streamflow is derived from groundwater, that is the mean infiltration is assumed to be equal to the mean flow, and infiltration is equal to effective precipitation. To derive values of monthly recharge the monthly values of effective precipitation were multiplied by a factor of 1.32 (280 mm year^{-1}/212 mm year^{-1}) for the western area and 1.11 (235 mm year^{-1}/212 mm year^{-1}) for the eastern area.

The final step in estimating the recharge times series was to estimate the transit time of the infiltration through the unsaturated zone. The catchment transit times were optimised during the calibration procedures.

A.5 CALIBRATION OF THE ASM MODEL

The parameters of the ASM model were optimised against observed groundwater levels and observed streamflow. The hydraulic conductivities were calibrated from steady state simulations, while the storativities and the transit times for the unsaturated zone were calibrated from dynamic simulations.

The simulated groundwater levels, derived from using K values calculated from the T values in Fig.3 (K equals T divided by 40 m) in a steady state simulation, ranged from about 80 m at the lowest point to more than 200 m in the north west. These are much higher than the observed mean values; this is shown in Fig.5. The distribution of steady state mean stream flow for various calibration methods is shown in Fig.7. From Fig. 7 it can be seen the mean flows from the upper western catchment are higher than the observed values whilst the flows in the south east of the catchment are lower.

The first approach to calibration was to calibrate K values by optimising the simulated groundwater levels based on the observed values, using an automatic least squares approach, the simulated average groundwater potential map is given in Fig 8. which shows a good fit

between the observed and simulated maps. The optimized K values, found by minimizing the sum of squared deviation between the simulated and observed groundwater levels in each grid cell, vary from $4x10^{-5}$ m s^{-1} ($T = 1.6x10^{-3}$ m^2 s^{-1}) near the periphery of the catchment to more than $3x10^{-3}$ m s^{-1} ($T = 1.2x10^{-1}$ m^2 s^{-1}) in the valley, which are an order of magnitude higher than the values shown in Fig. 3. The flow distribution was, however, still erroneous, with insufficient water flowing from the upper western catchment. This distribution was unaffected by any variation of the leakage coefficient. The erroneous flow distribution could either be due to uncertainty in defining the average groundwater levels or wrong model assumptions.

By manual calibration simultaneously based on both flow values and groundwater levels a final conductivity distribution was found. These values range from $2x10^{-5}$ m s^{-1} ($T = 8x10^{-4}$ m^2 s^{-1}) to $1x10^{-3}$ m s^{-1} ($T = 4x10^{-2}$ m^2 s^{-1}), which are 2-5 times higher than the values shown in Fig. 3 (the highest multiplication factor relating to the peripheral areas). Similar values were found by Morel (1980), who also used a finite difference model calibrating the transmissivity by an inverse method. The resulting groundwater levels using the K values from this manual calibration exceed the groundwater levels in Fig.5 by 5-10 m in the western areas, Fig.9., however the mean flow distribution was deemed to be the closest fit to the distribution of observed mean flows within the catchment (Fig. 7).

With the calibration of the hydraulic conductivity completed, the transit time in the unsaturated zone and the storativity values were calibrated from non steady state simulations. The amplitude of the seasonal variations in streamflow are influenced by both parameters, whereas transit time only determines the phase of the flows.

Good results were found by introducing a transit time of two months in the peripheral areas, one month in the middle area, and no delay in the valleys. The calibrated storativity was 1.5 % in the peripheral area above approximately 160 metres and 3 % in the remaining area. The boundaries between the areas follow the contour lines of the topography. Comparisons between the simulated and observed streamflows are presented in the form of the annual flow duration curve and a part of the simulated hydrograph for the station at Shaw in Figs. 10 and 11 respectively.

Well hydrographs were monitored for three wells in the catchment; SU38/51 up on the Downs, SU37/24 in the Lambourn valley and SU47/17 on the periphery of the catchment at the top of the Winterbourne, Fig. 12. Examples of the hydrographs in Figs. 13 to 15 show little difference in the quality of fit to the observed data between the two calibration approaches.

A.6 PREDICTING THE LOW FLOW RESPONSE OF GROUNDWATER ABSTRACTIONS

The long term flow response was investigated by simulating constant and seasonal abstractions in different locations and with different abstraction rates. It took approximately four years for the model to reach equilibrium, and so the first four years of simulation were omitted from the analysis.

The locations of the hypothetical abstractions are shown in Fig. 4. The distances from the stream are 0.5 km, 1 km, 2 km and 3 km. The transmissivity decreases with increasing distance from the stream.

For each simulation the monthly stream depletion factor (SDF) was calculated as

$$SDF = \frac{\Delta q_d}{Q} \quad , \qquad (4)$$

where Δq_d is the difference between the simulated natural flow and the flow influenced by the abstraction, and Q is the pumping rate. For seasonal abstractions the monthly pumping rate is used to define the SDF even in those months when pumping ceases.

The results of the analysis have shown that:

1. The SDF is independent of the pumping rate up to at least 500 $m^3 hour^{-1}$.

2. A constant continuous abstraction results in seasonal variation of the SDF, (Fig. 16). lines have been drawn between the monthly values to illustrate the different SDF regimes more easily. The variation is small for abstractions near the stream. For the abstraction 3 km from the stream the monthly mean SDF varies from 0.89 to 1.13, (Fig. 17). The SDF is largest when the groundwater levels and the stream flows are high, which is due to a more rapid flow routing (large hydraulic gradients). The Figure also illustrates the relative decrease in aquifer storage in the summer to supply the excess of groundwater abstraction over stream depletion. Conversely in the winter there is a relative increase in storage when the streamflow depletion is greater than the abstraction.

3. The introduction of a seasonal abstraction results in a seasonal depletion. The seasonal depletion depends primarily on the duration of the abstraction and the distance from the stream, not the time of year when the abstraction occurred.

The dependence on distance is illustrated in Fig. 18, which shows the monthly variation in SDF for a six month abstraction period from April to September at the four abstraction locations. From Fig. 18 it is seen that as the distance from the stream increases the damping of the amplitude of the monthly variation in SDF. As a result, although the total mass depleted from the stream is independent of the distance from the stream, the monthly SDF is more evenly distributed throughout the year.

The monthly variation in SDF for abstraction scenarios of two months durations are illustrated in Fig. 19 for the locations at 0.5, 1 & 2km from the stream. For the location at 0.5 km from the stream the monthly variation in SDF is plotted for three seasonal scenarios; when the 2 month period occurs in December-January, April-May & August-September. From these scenarios it can be seen the magnitude and variation of the monthly SDF is independent of the seasonality of the abstraction. For clarity, only the variation in monthly SDF for the abstraction occurring in April-May is shown for the locations at 1 & 3 km from the stream. As the distance form the stream is increased the variation in SDF is damped, as seen for the six month abstraction scenarios in Fig. 18, however for the shorter 2 month abstraction scenario there is a shift in the occurrence of the peak SDF from June to July, ie to the month after the abstraction has stopped.

It should be noted that the definition of SDF, whilst enabling easy calculation of the numerical impact on the stream, does not conserve mass for intermittent pumping scenarios and thus does not allow for easy numerical comparison between scenarios.

The modelling work of Rushton *et al.* (1992) considers the impact in August 1976 of target abstraction regimes at three sites (the sum of the three constituting a continuous time dependent abstraction, peaking in the summer months) on the Oolitic Limestone headwater rivers of the River Thames. The abstraction points were at least 3 km from the nearest stream. Adjusting for vertical flow from a minor aquifer the presented results indicate an overall approximate SDF of 0.85 during the August low flow period. Whilst the hydrology of the Oolitic limestone is very different to that of the Chalk, it is interesting to note that this SDF is very similar to the 0.89 SDF observed for a continuous abstraction at 3 km from the Lambourn stream in this study.

During the 1976 test period of the River Candover Groundwater Augmentation scheme (Giles *et al.*, 1988) a group of six wells at a distance of 7 km from the Candover headwaters were pumped at a combined rate of 1155 m^3/hr for a period of six months from May to October. By August the nett gain to the stream had been reduced to 70%, giving an SDF of 0.3. However, 20% of the total nett gain had been derived from an adjacent catchment. Assuming this occurred during the last three months of pumping the approximate adjusted SDF would be 0.6. The Candover is a chalk catchment with a higher transmissivity and a lower storativity than the Lambourn catchment. Thus, for a given distance the impact of a specific transient abstraction regime on a stream would be observed earlier and would be less diffuse (Oakes & Wilkinson; 1972) in the Candover catchment compared with the Lambourn catchment. In view of this the results from the Candover scheme are not inconsistent with the results obtained for the 6 month abstraction period during this study.

Based upon the impacts described it is possible to summarize the impacts on river flow regime as follows:

A constant abstraction will result in a minor seasonal variation in the amplitude of stream depletion. The amplitude increases with the distance from the stream. For a given distance from the stream, the smallest depletion rates occur during periods of low flow. The degree of influence that a constant continuous abstraction exerts on the stream at any point in time is inversely proportional to the stream flow at that point in time, although this variability is relatively small in comparison to the pumping rate. This means that low flow measures such as the 95 % exceedance and the annual minimum discharge will be reduced by the abstraction rate multiplied by the SDF, which is less than but close to 1.00. Fig. 13 shows the flow frequency curve of the annual minima for the natural stream flow and the stream flow influenced by constant abstraction rates of 500 m^3 hr^{-1}. The effect on the annual minima is greatest for the abstraction nearest to the stream. This is illustrated in Fig. 20 which also shows the almost constant influence from year to year.

The impact of a seasonal abstraction will depend primarily on the abstraction rate, the distance from the stream and the time of the year the abstraction takes place. In contrast to a constant abstraction, the influence of a seasonal abstraction on low flow statistics is more dependent on the year to year variability of low flows in both their timing and magnitude and how they relate to the timing and magnitude of the depletion.

As the distance from the stream increases the monthly variation in the SDF for a annual periodic, intermittent abstraction is damped by the storage properties of the increased aquifer volume between the abstraction location and the stream, as the distance tends to infinity the influence on the stream will tend to that of a constant abstraction at a rate equal to the mean abstraction rate over the whole year.

In the case of annual minimum discharges the month of the minimum is critical in terms of the direct effect of depletion. Annual minima will be reduced more severely when the month with the natural minimum is coincident with the month of the maximum depletion, (Fig. 21). Thus in Chalk streams such as the Lambourn where the minimum flow normally occurs in October or November the maximum impact of a seasonal abstraction would be from a borehole close to the stream with a maximum abstraction in September and October.

A.7 CONCLUSIONS

The influence of long term groundwater abstractions on a natural flow regime has been investigated using a two dimensional regional groundwater model. The model was calibrated on observed groundwater levels and stream flow. The calibrated values of hydraulic conductivity and storativity were found to be in accordance with values found from field measurements and calibration of other numerical models. After the model was calibrated it was possible to simulate the natural flow at the gauging stations.

The analysis of the simulations showed that the stream depletion with a constant abstraction depend on the abstraction rate, the distance from the stream and discharge. The depletion of a seasonal abstraction depends on the abstraction rate, the distance from the stream, the duration of the abstraction, but not the time of the year. The influence of a seasonal abstraction on low flows depends on the factors cited above and the natural low flow variability.

A.8 REFERENCES

Connorton, B.J. and Reed, R.N. (1978). A numerical model for the prediction of long term well yield in an unconfined Chalk aquifer. *Quart. J. Eng. Geol.* 11, 127-138.

Giles, D.M., Lowings, V.A. and Midgley, P. (1988). River regulation by seasonal groundwater abstraction: the case of the River Itchen. *Regulated rivers: research and management*, vol.2, 335-347 (1988).

Gustard, A., Bullock, A. and Dixon J.M (1992). Low flow estimation in the United Kingdom. *Institute of Hydrology report*, no. 108.

Hardcastle, B.J. (1978). From concept to commissioning. *Thames Groundwater Scheme, Institution of Civil Engineers*, 5-31.

Kinzelbach, W. and Rausch, R. (1989). Aquifer Simulation Model "ASM", Documentation. Kassel Universität, Kassel, FRG, 49 p.

Morel, E.H. (1980). The use of a numerical model in the management of the Chalk aquifer in the upper Thames basin. *Quart. J. Eng. Geol.* 13, 153-165.

Oakes, D.B. and Wilkinson, W.B.(1972). Modelling of groundwater and surface water systems, I. - Theoretical relationships between groundwater abstraction and baseflow. *Water*

Resources Board, 1972.

Owen, M., Connorton, B.J. and Robinson, V.K. (1977). The hydrogeology of the Thames ground water scheme. In: *International Association of Hydrogeologists, Memoires*, Vol. XIII, part I, Birmingham Congress, UK, D20-D31.

Owen, M. and Robinson, V.K. (1978). Characteristics and yield in fissured Chalk. *Thames Groundwater Scheme, Institution of Civil Engineers*, 33-49.

Prickett, T.A. and Lonnquist, C.G. (1971). Selected Digital Computer Techniques for Groundwater Resource Evaluation. *Illinois State Water Survey*, Bulletin 55, 62 p.

Rushton, K.R., Connorton, B.J. and Tomlinson, L.M. (1989). Estimation of the groundwater resources of the Berkshire Downs supported by mathematical modelling. **Quart. J. Eng. Geol.** 22, 329-341.

Rushton, K.R., Owen, M. and Tomlinson, M.L. (1992). The water resources of the Great Oolite aquifer in the Thames Basin, UK. *J. Hydrol.* 132(1992), pp 226-248.

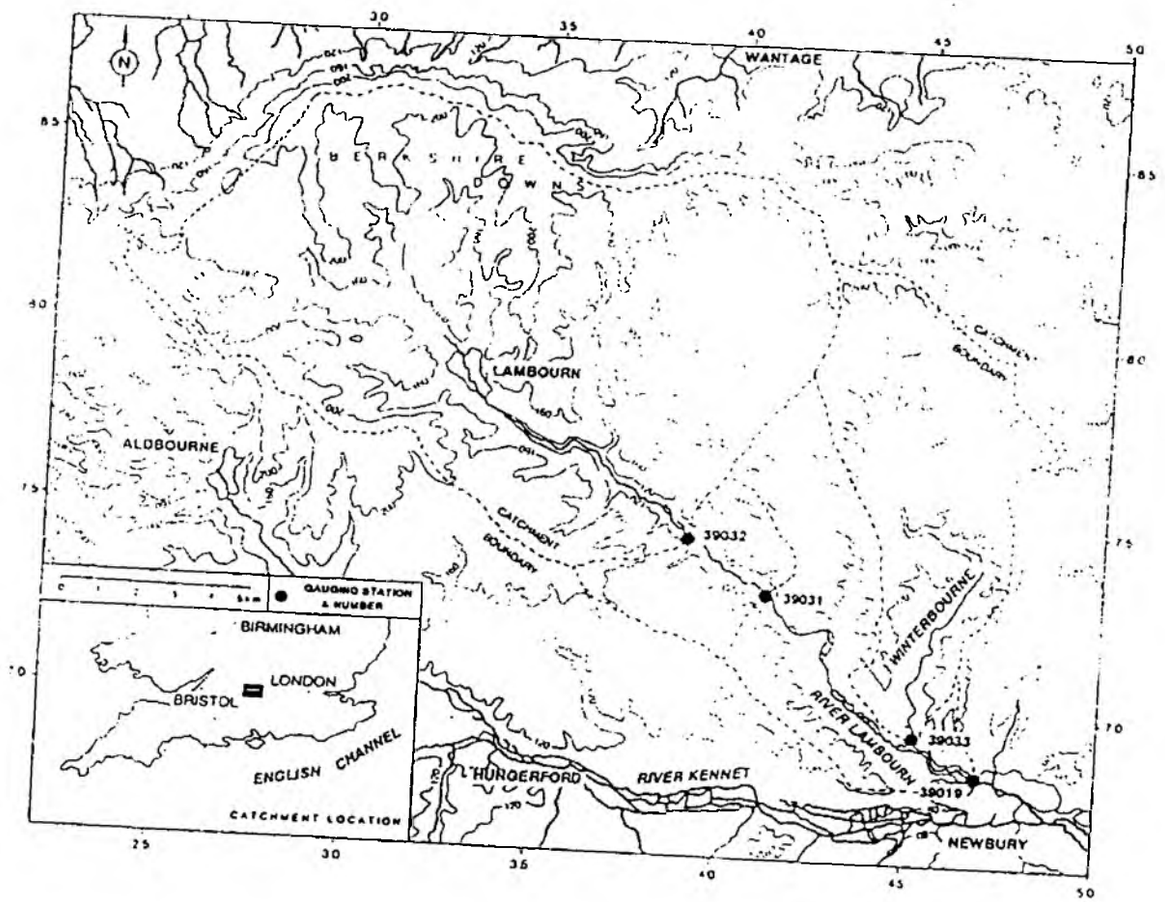

Fig. 1 The topographic catchment of the River Lambourn.

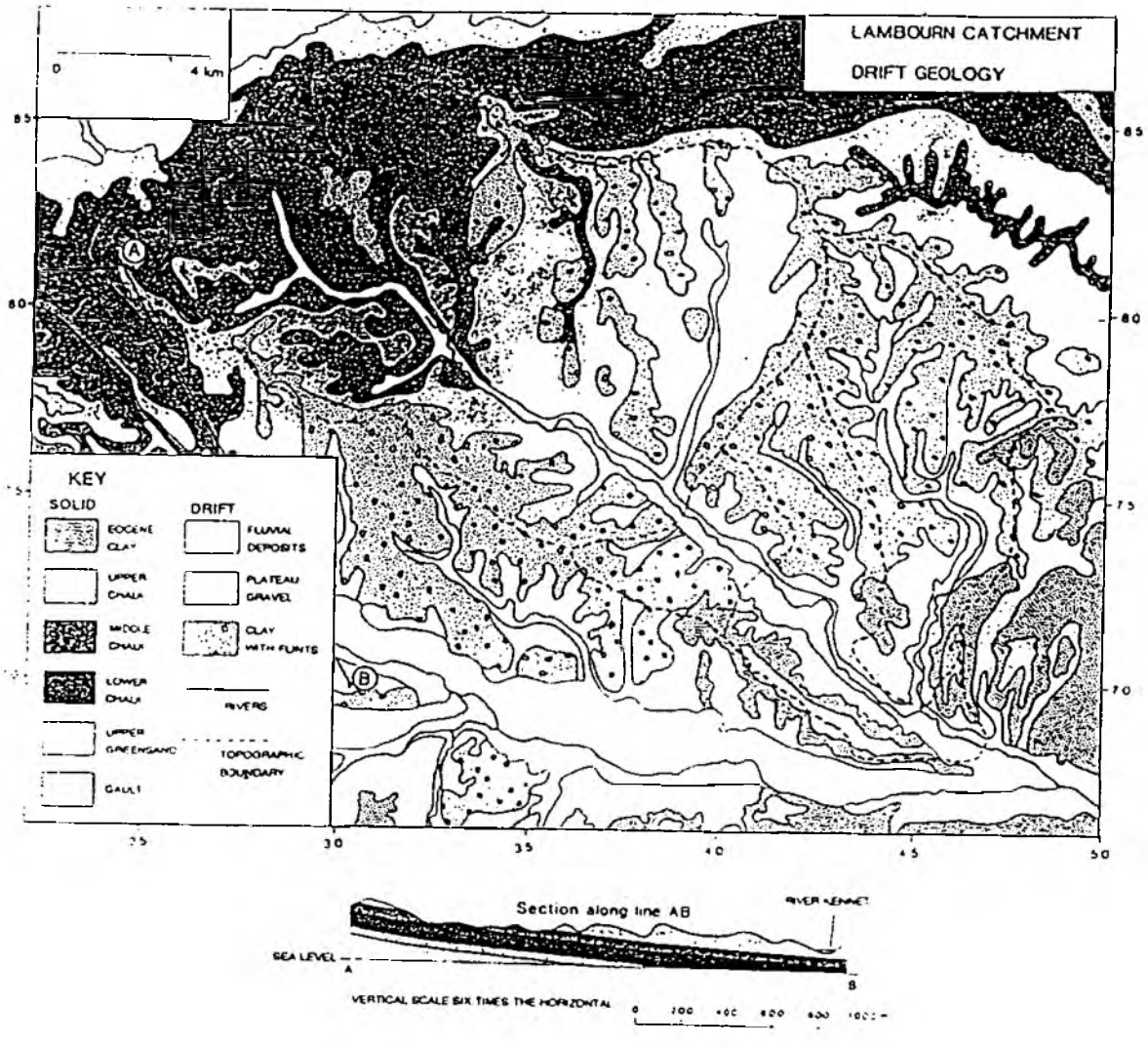

Fig. 2 The geology of the Lambourn catchment.

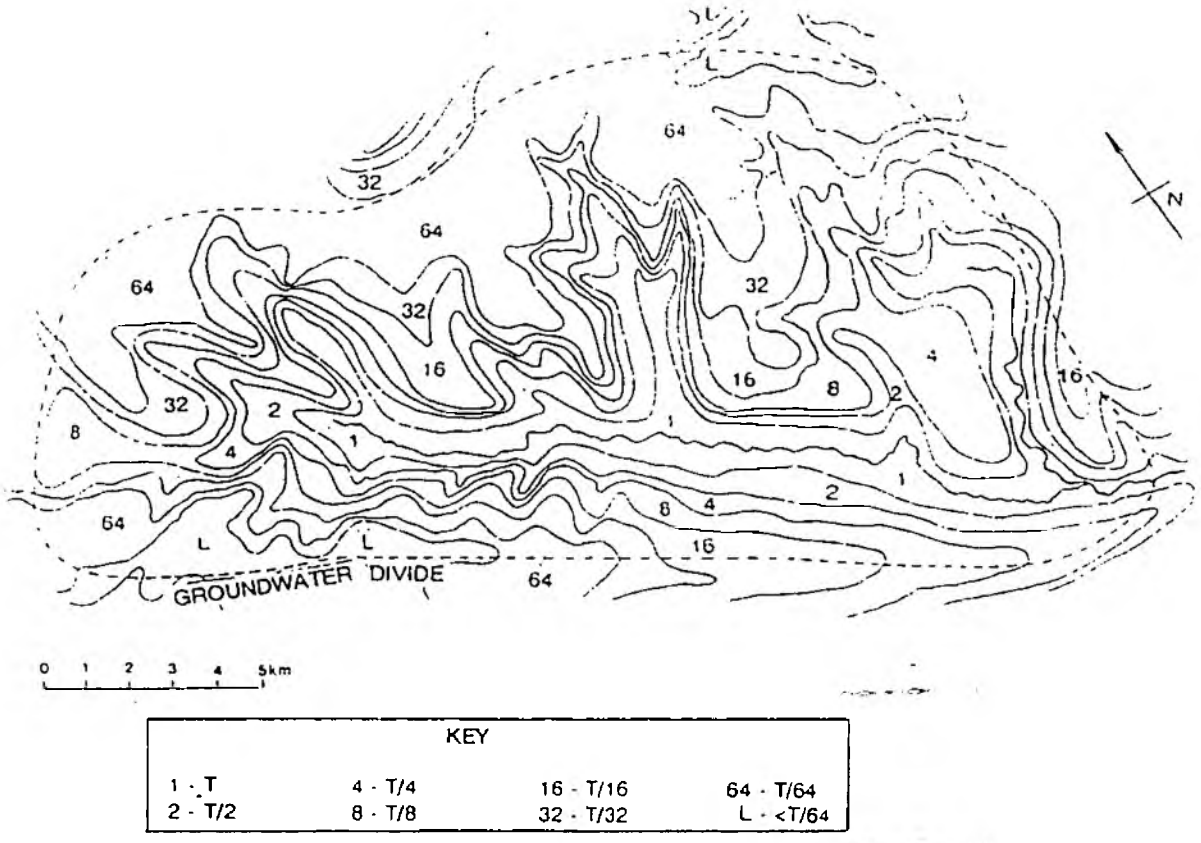

Fig. 3 Relative transmissivity distribution (after Owen and Robinson, 1978).

Fig 4. Model Representation of the Lambourn Catchment

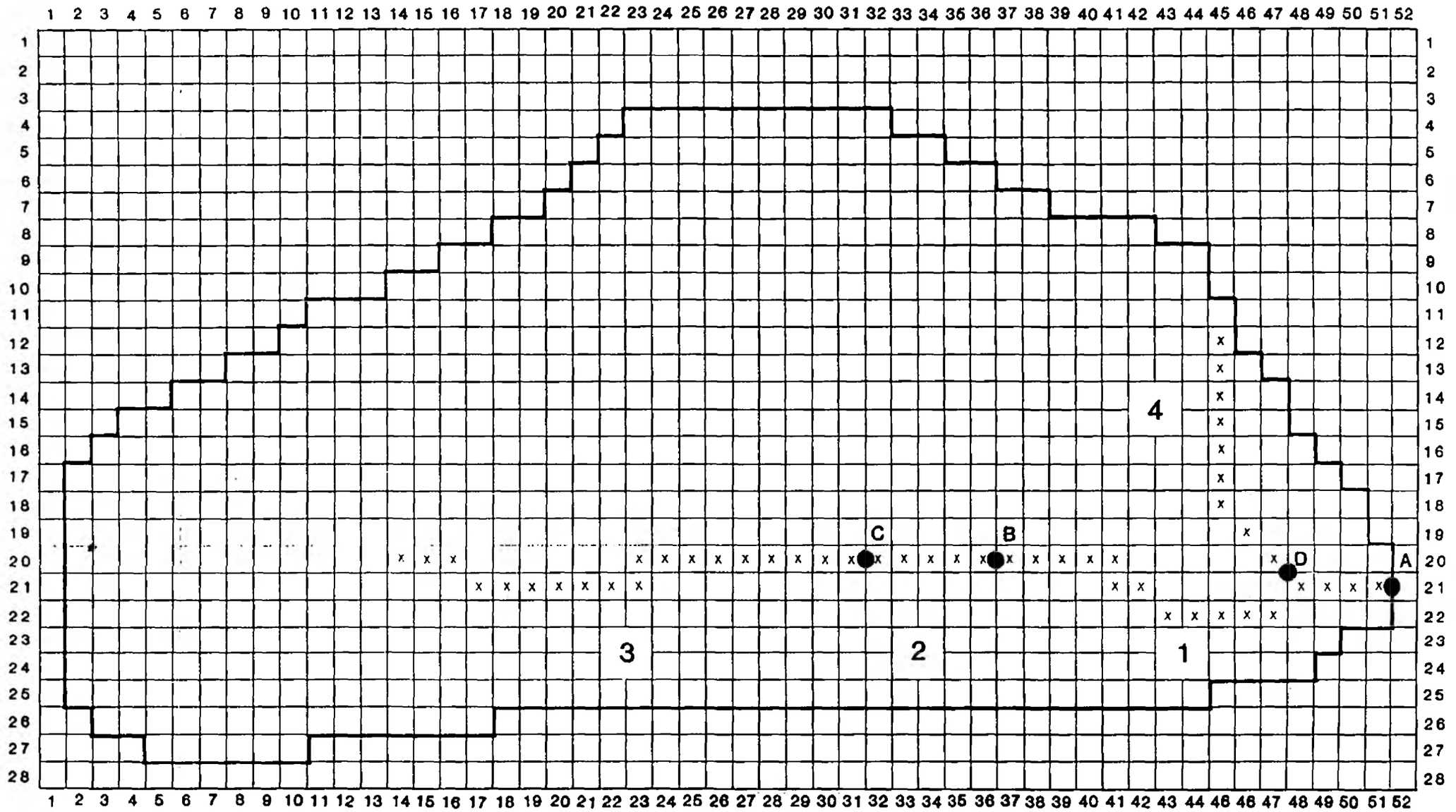

□ 0.5km x 0.5km

● Gauging Station

x Intermittent Stream

A. Shaw

B. Welford

C. East Shefford

D. Winterbourne

Fig 5. Simulated and Observed Groundwater Potential Observed Hydraulic Conductivity (K).

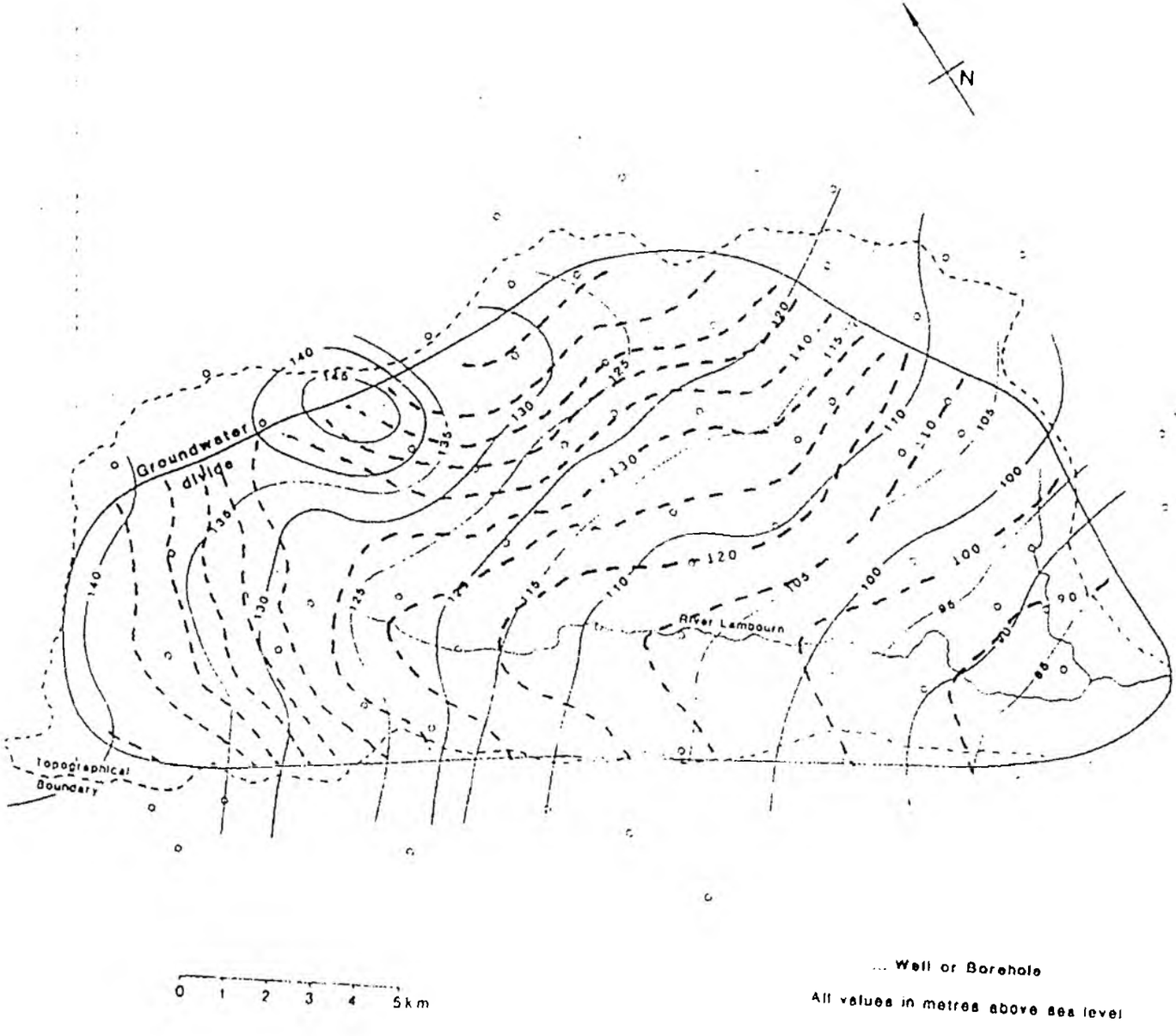

Fig 6. MEAN RECHARGE

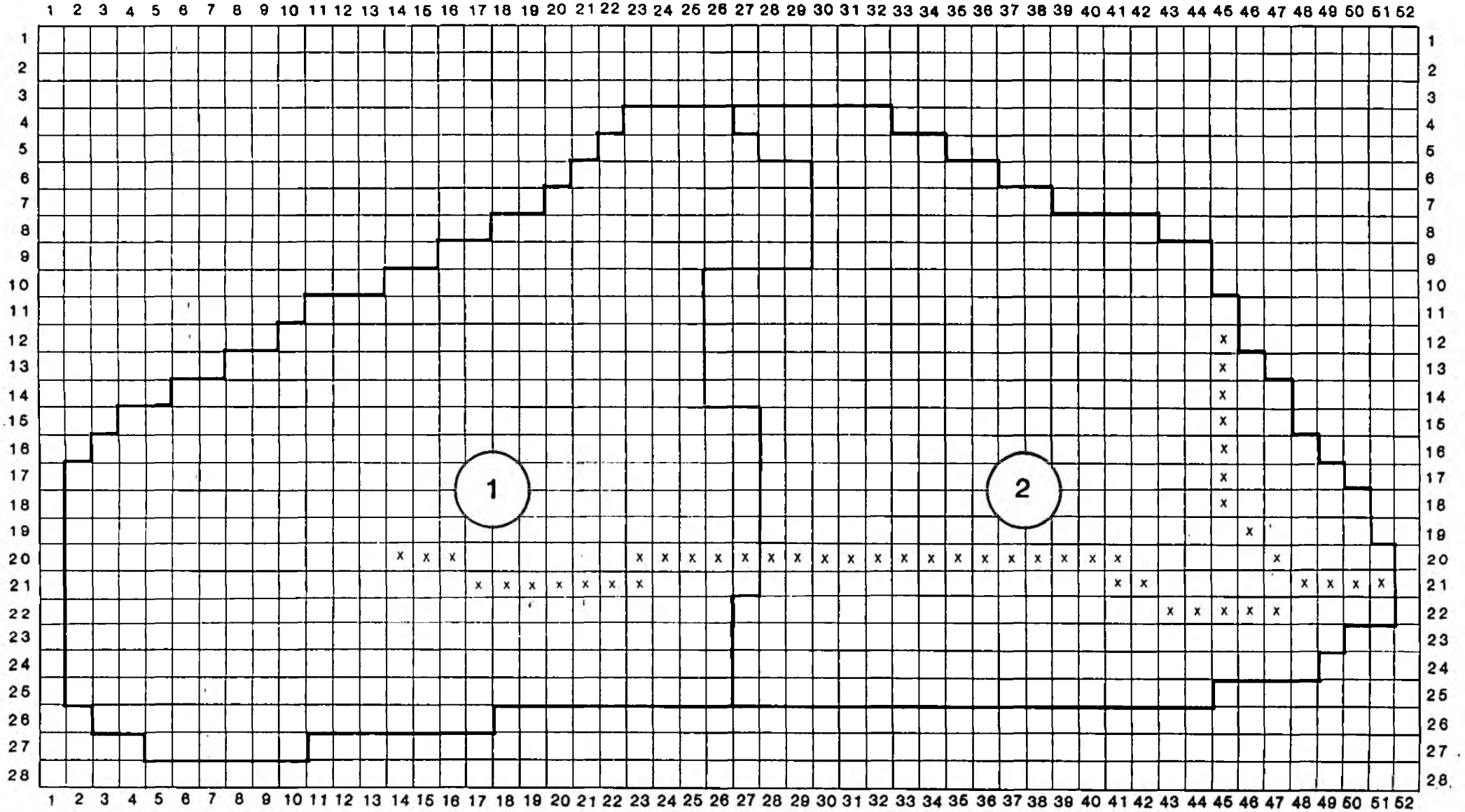

1. 280mm/year
2. 235mm/year

□ 0.5km x 0.5km

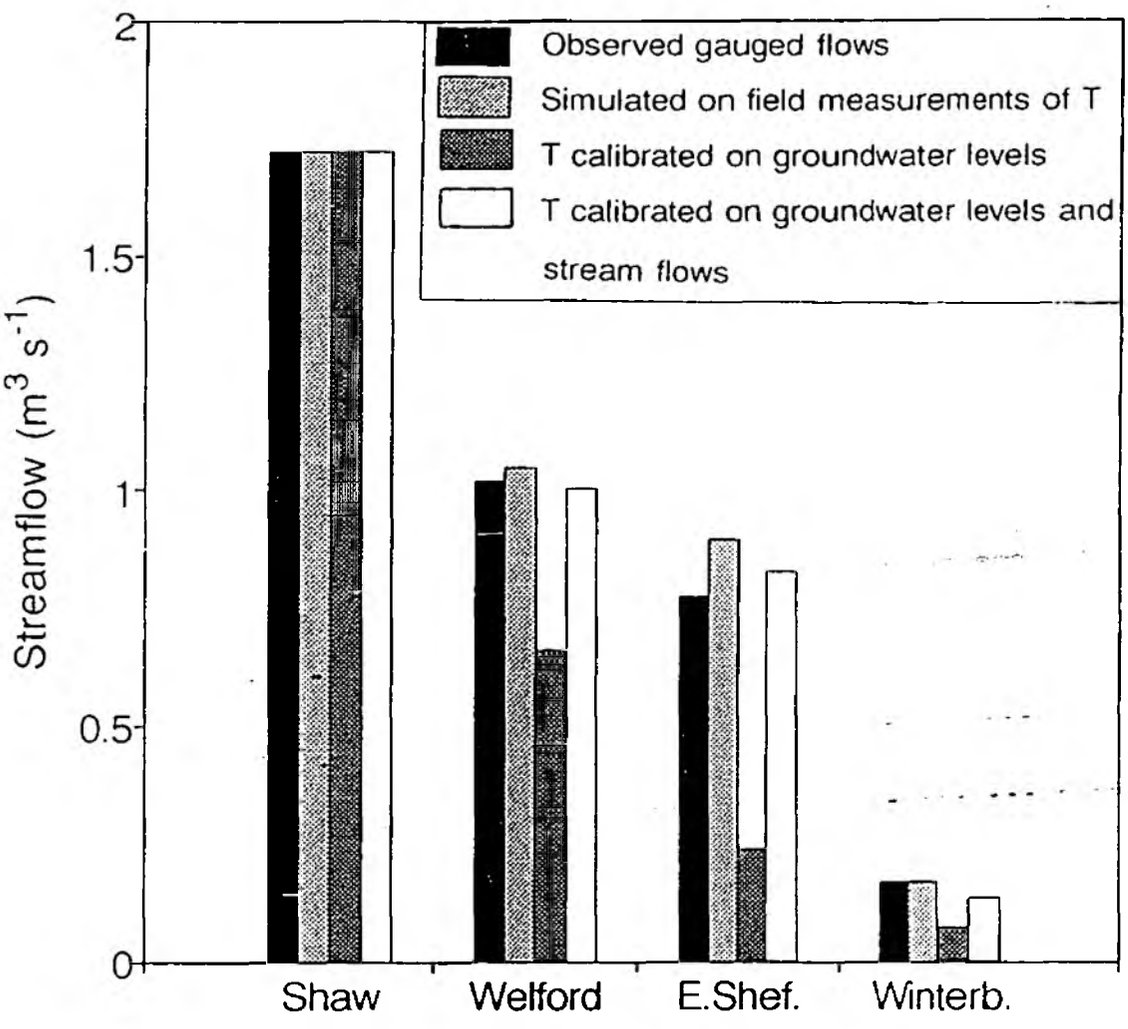

Fig 7. Observed and simulated mean flow distribution obtained from steady state simulations.

Fig 8. Simulated and Observed Groundwater Potential K Calibrated on Observed Groundwater Levels.

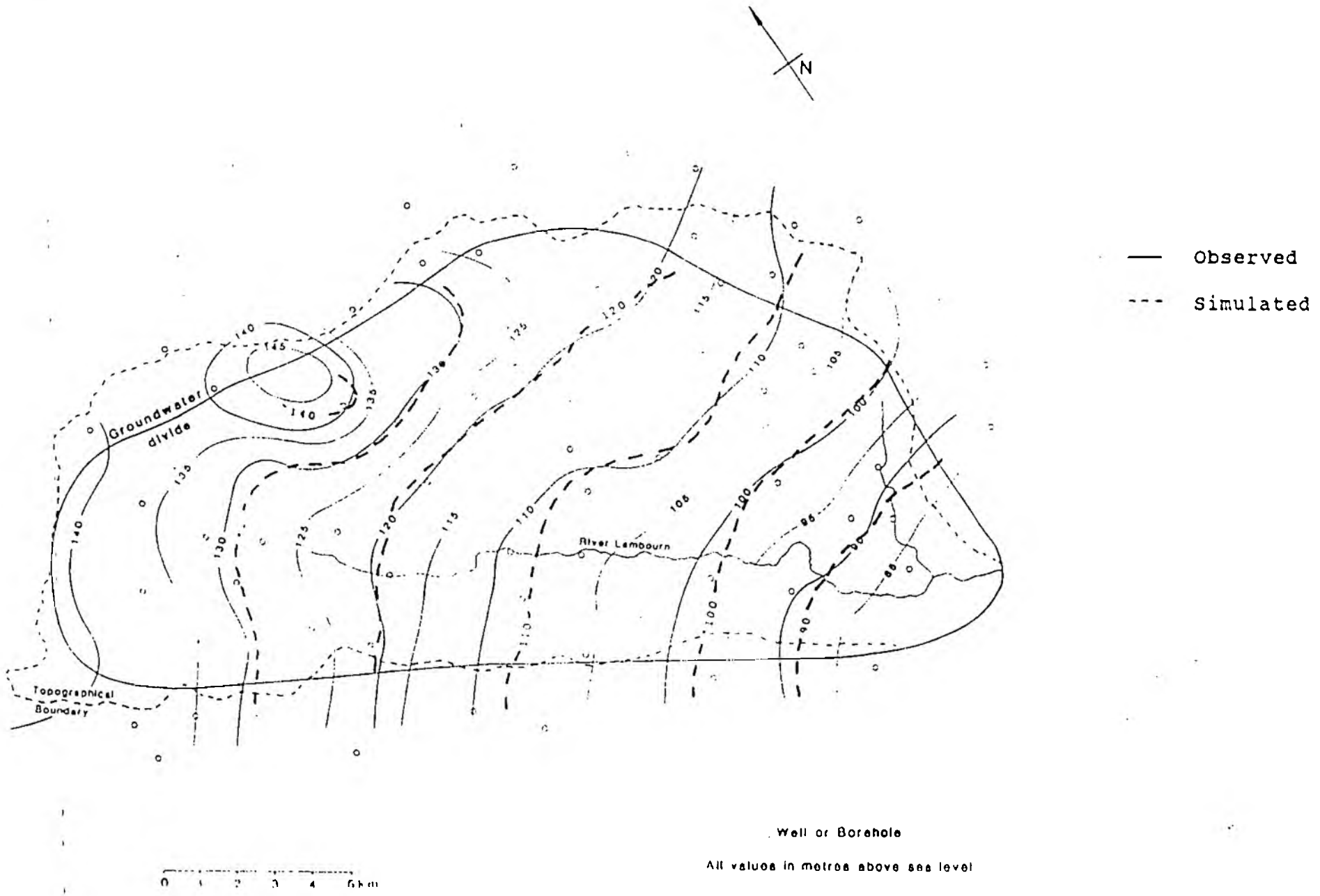

Fig 9. Simulated and Observed Groundwater Potential K calibrated on Groundwater Levels & Streamflow.

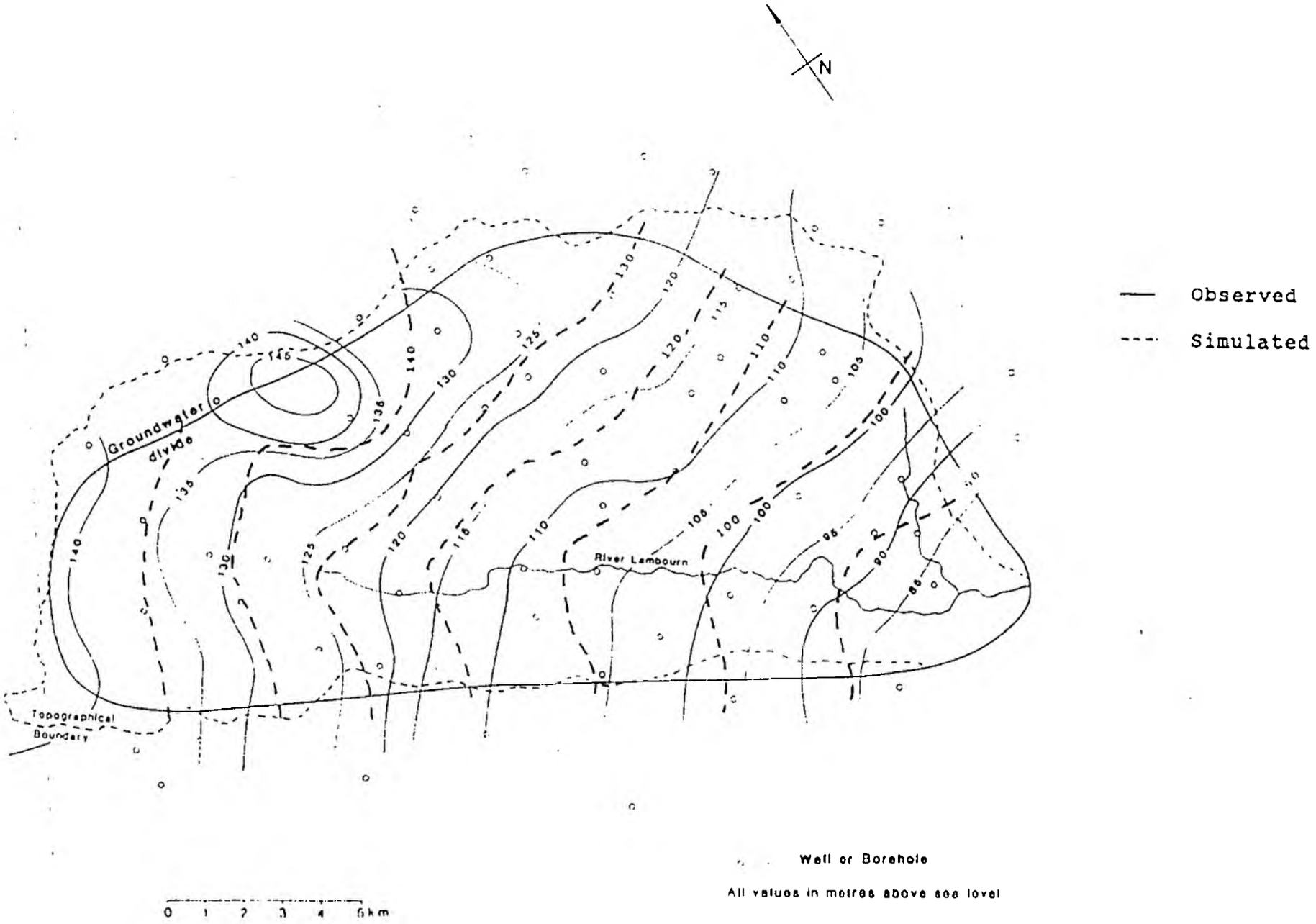

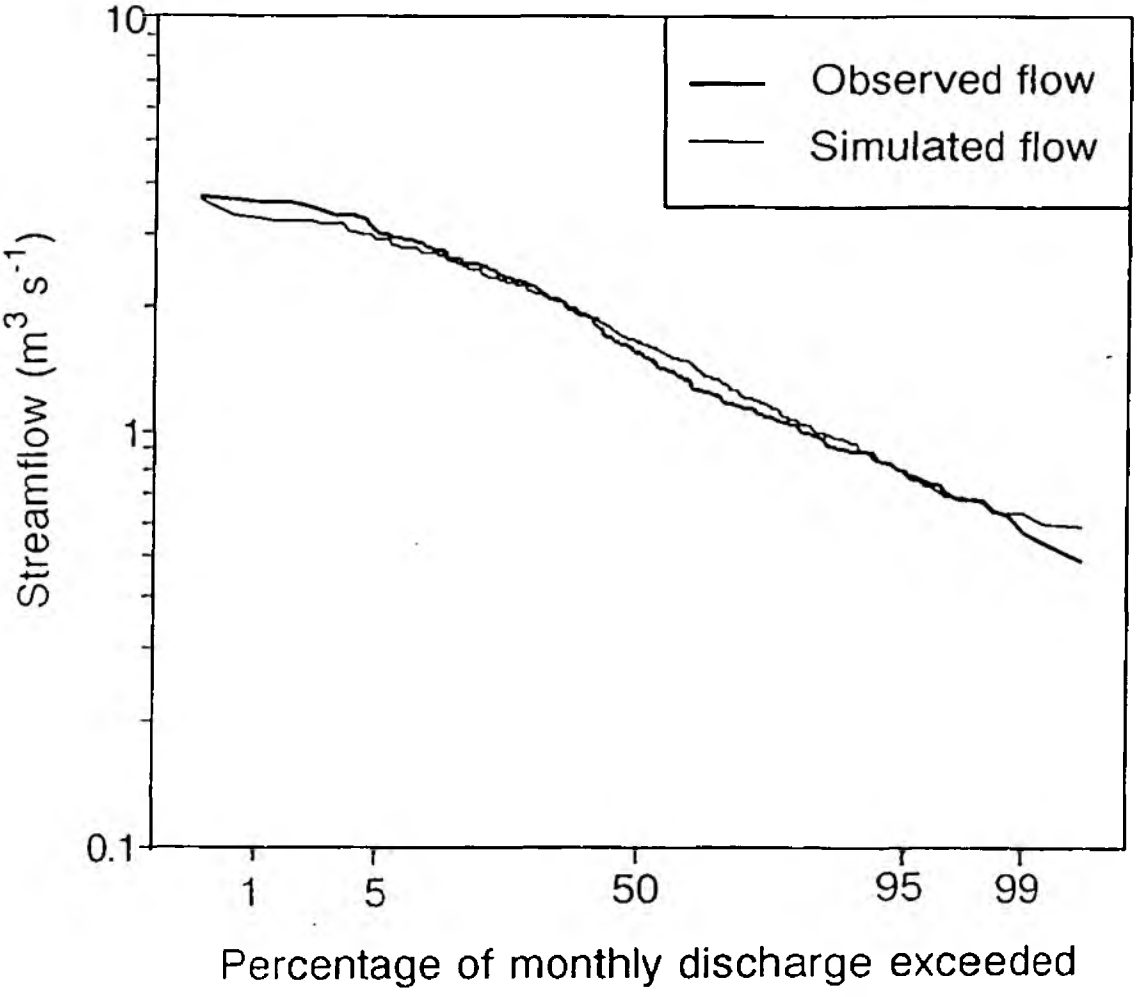

Fig 10. Observed and Simulated flow duration curve at Shaw.

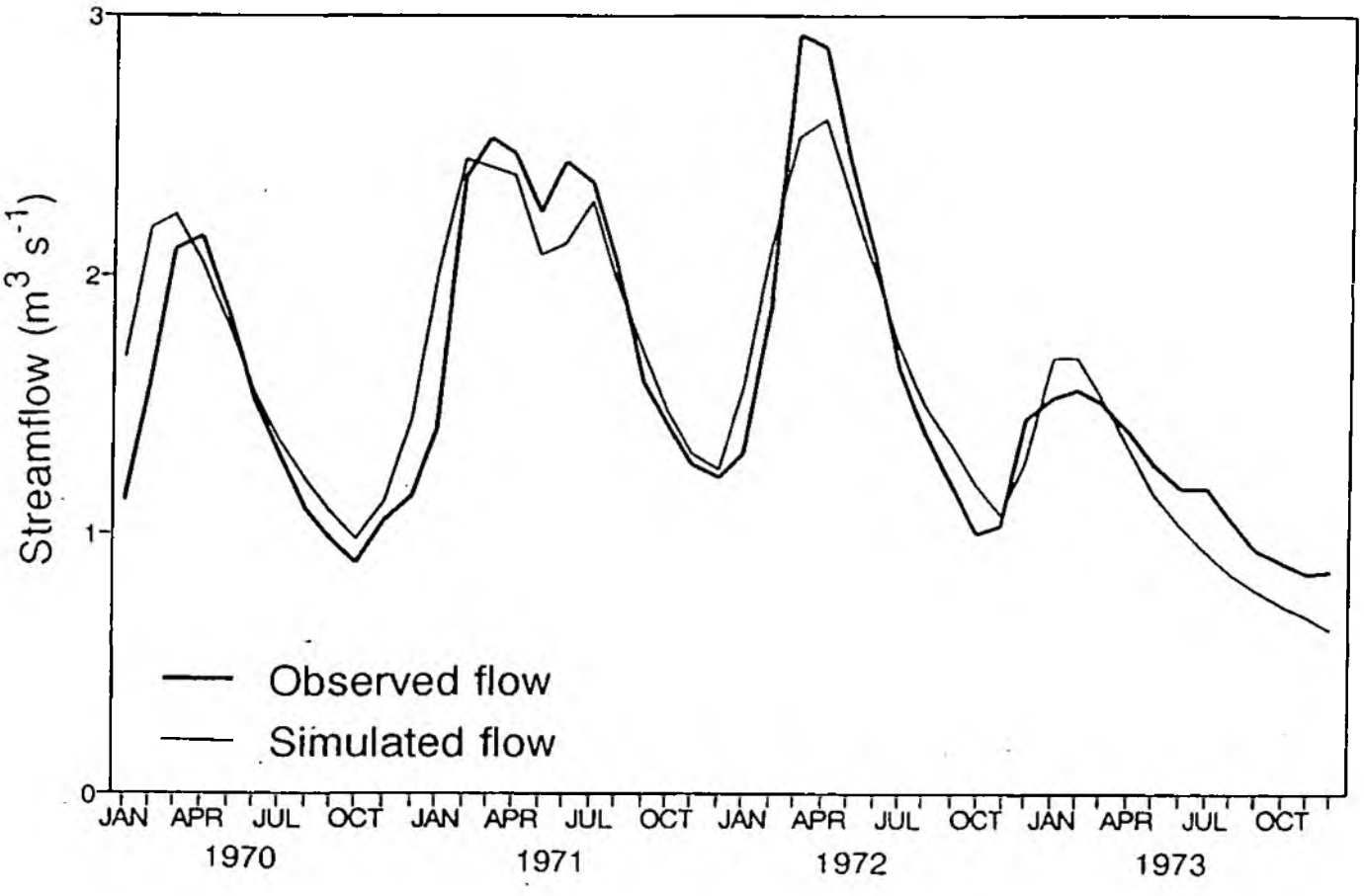

Fig 11. Observed and simulated hydrograph at Shaw for 1970-1973.

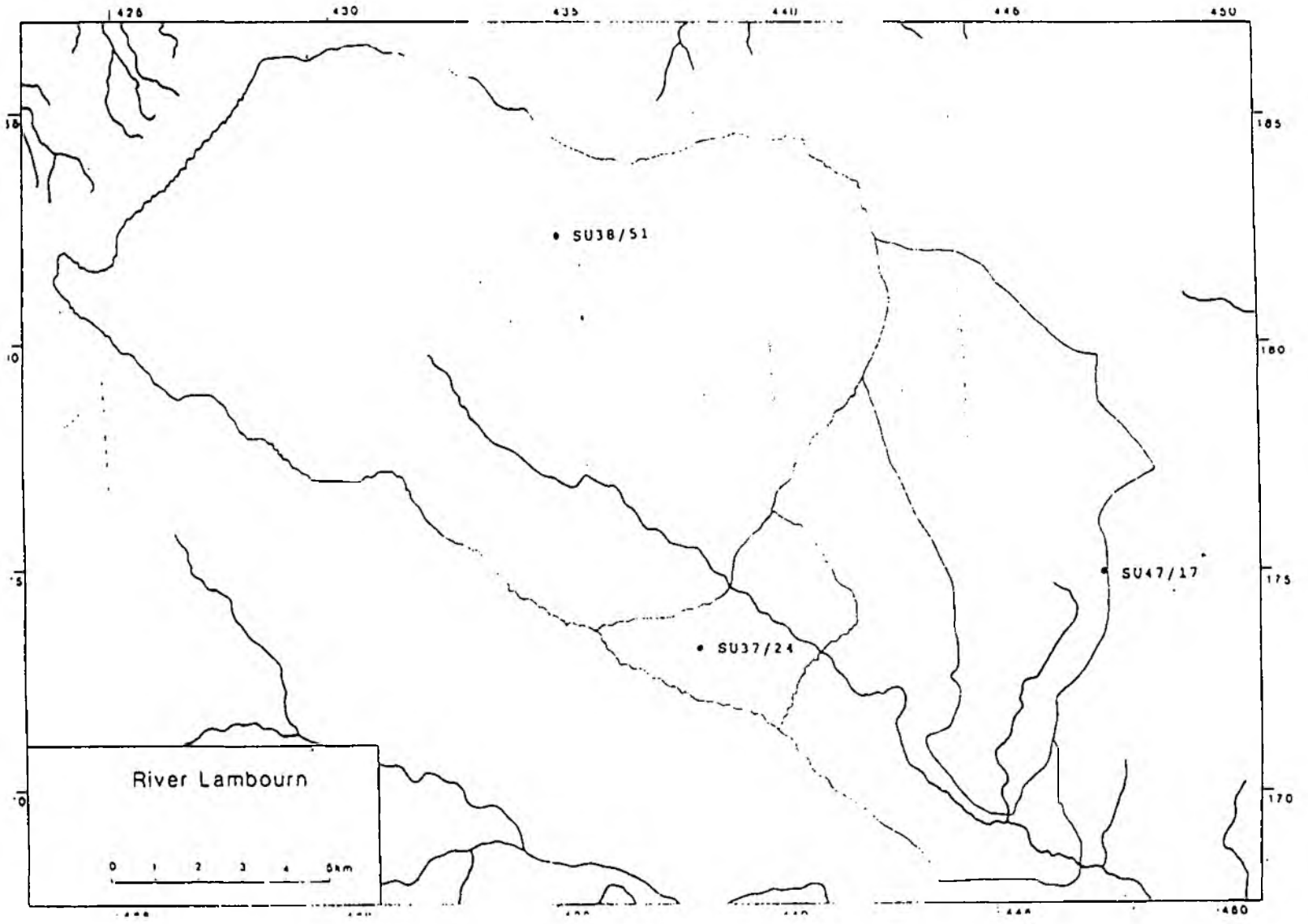

Fig 12. Location of the observation wells.

Fig 13. Water Levels at Down End Cottage - Chievley Well No: SU47/17.

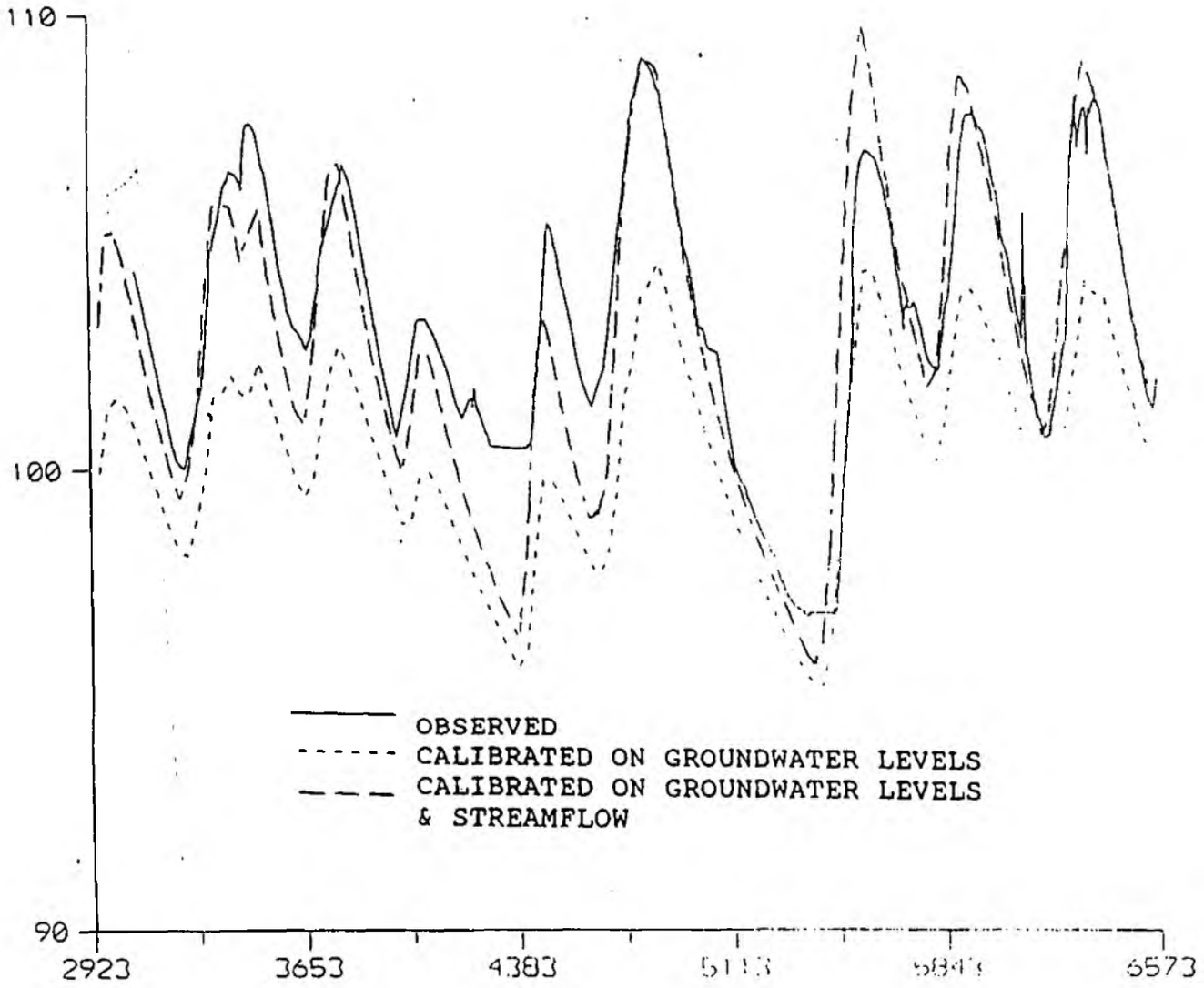

Fig 14. Water Levels at Oakhanger Park - (Disused) Well no: SU37/24.

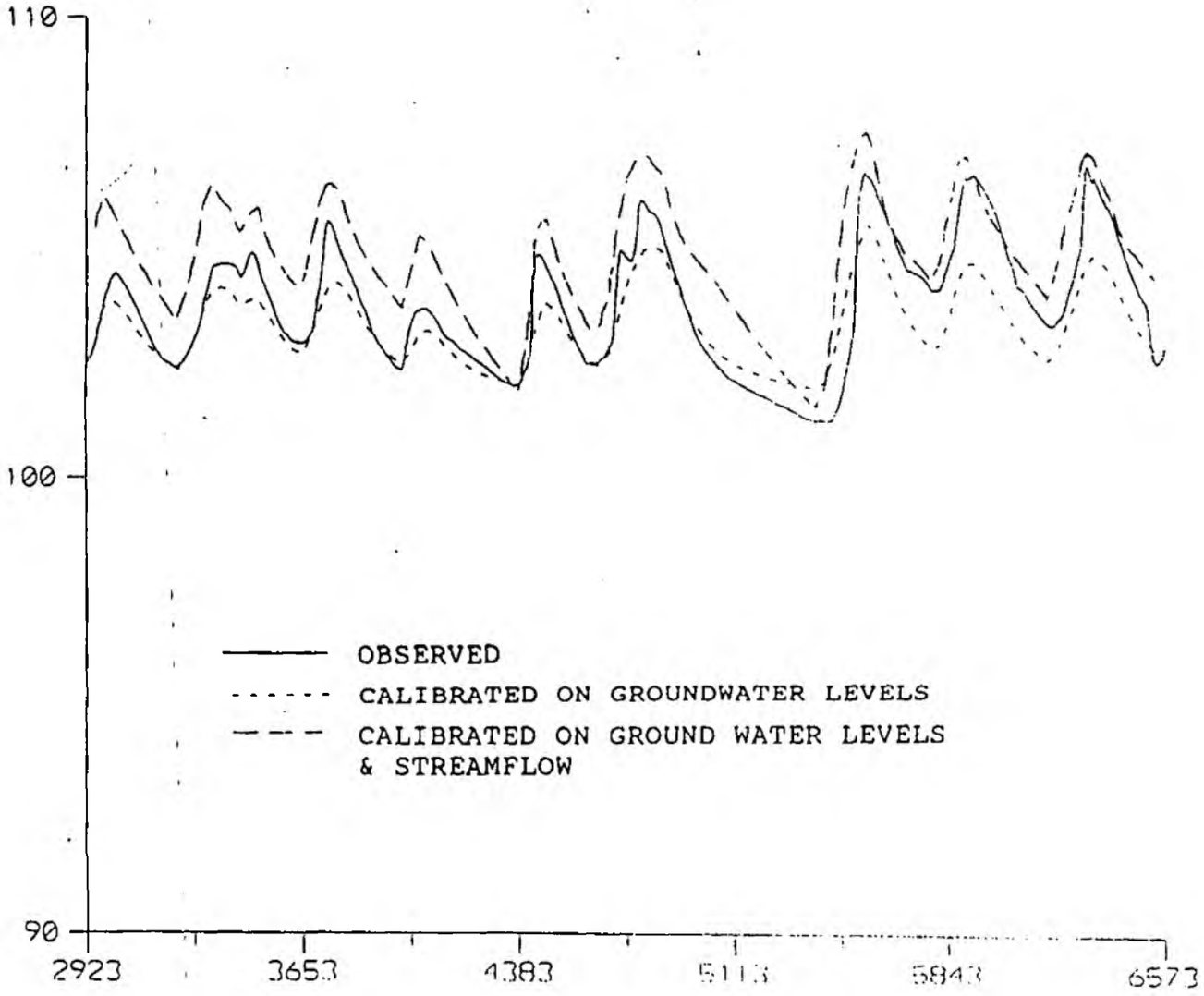

Fig 15. Water Levels at Stancombe Farm - Lambourn Downs Well No: SU38/51.

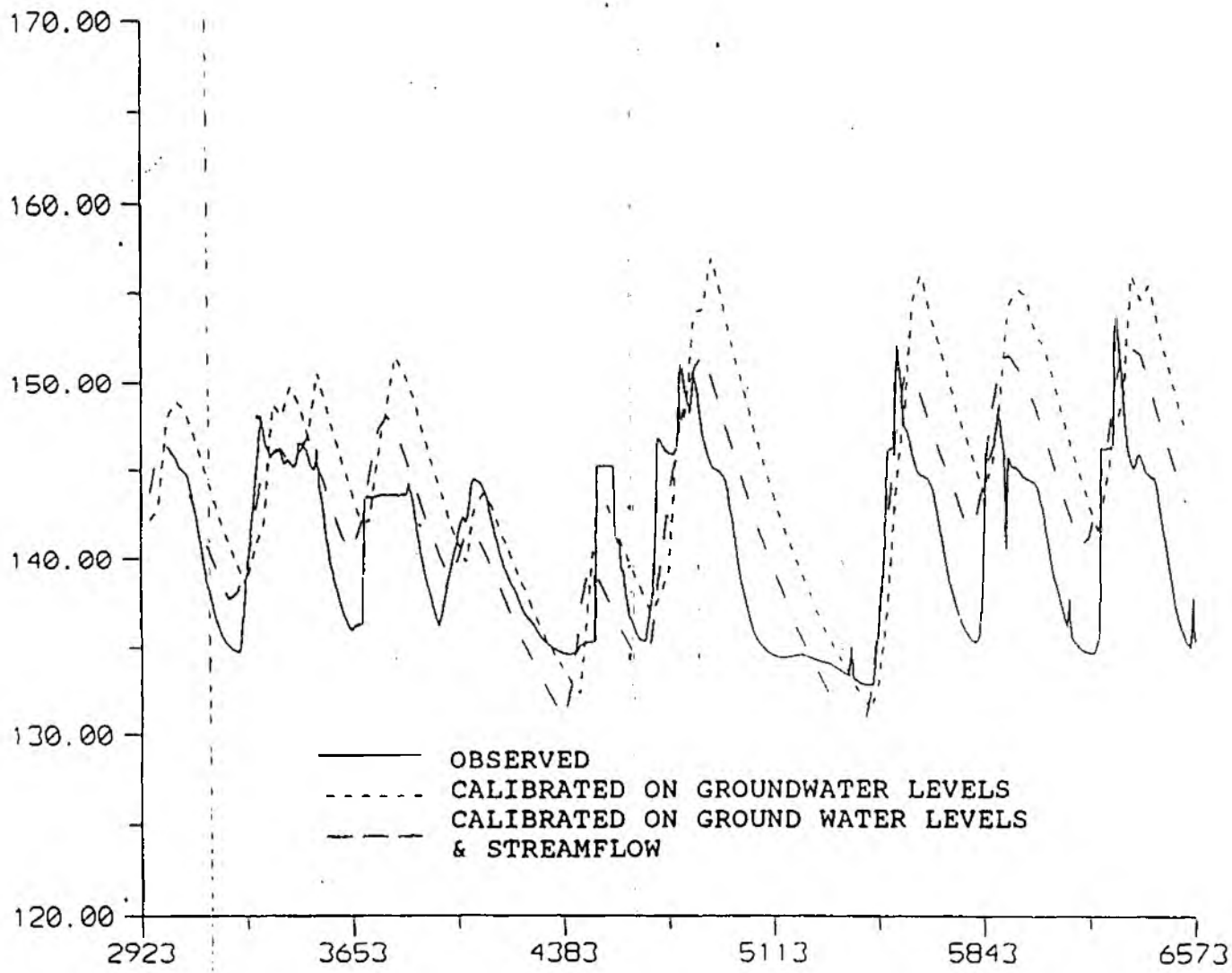

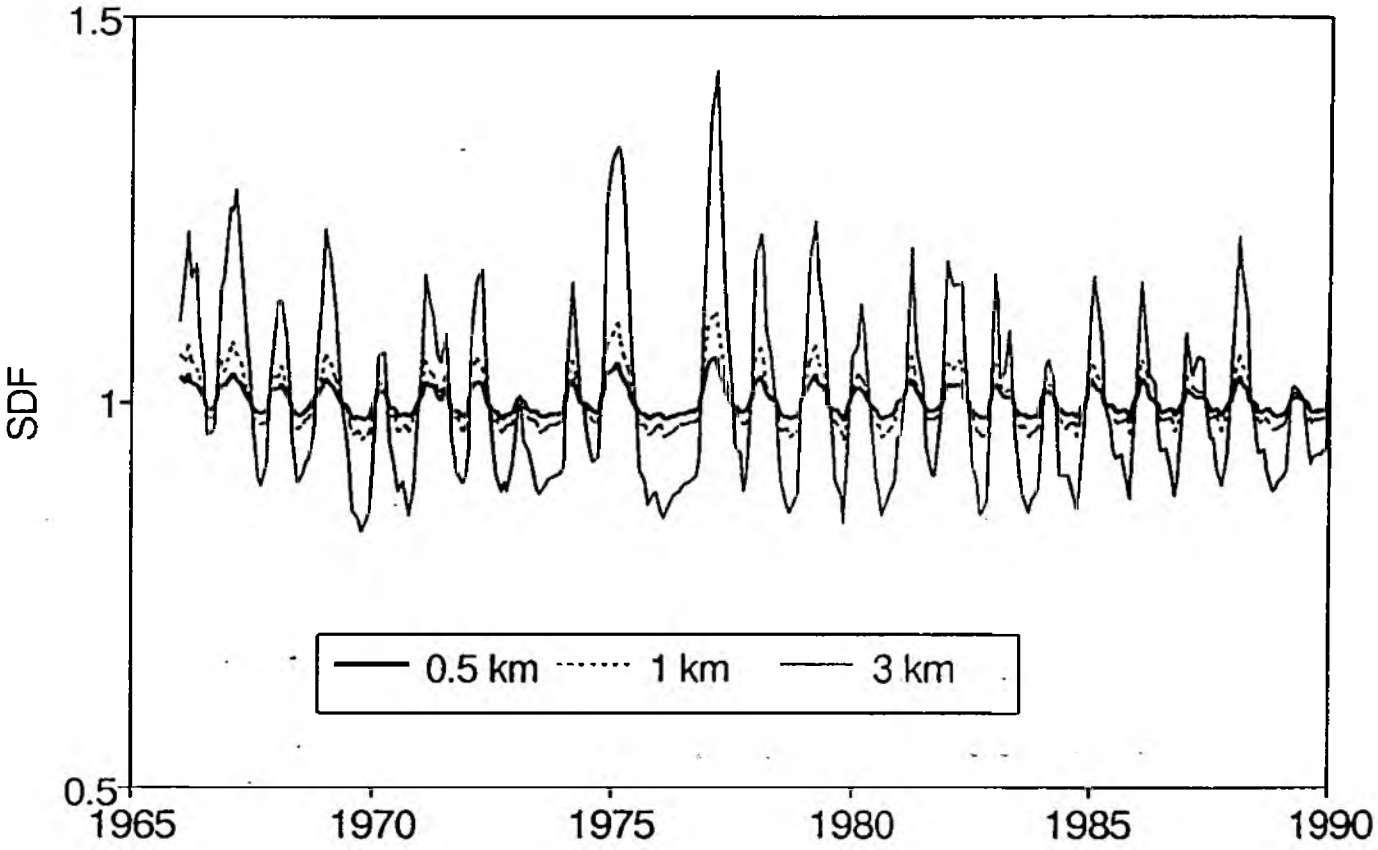

Fig 16. The variation of the stream depletion factor (SDF) for different locations with constant abstractions.

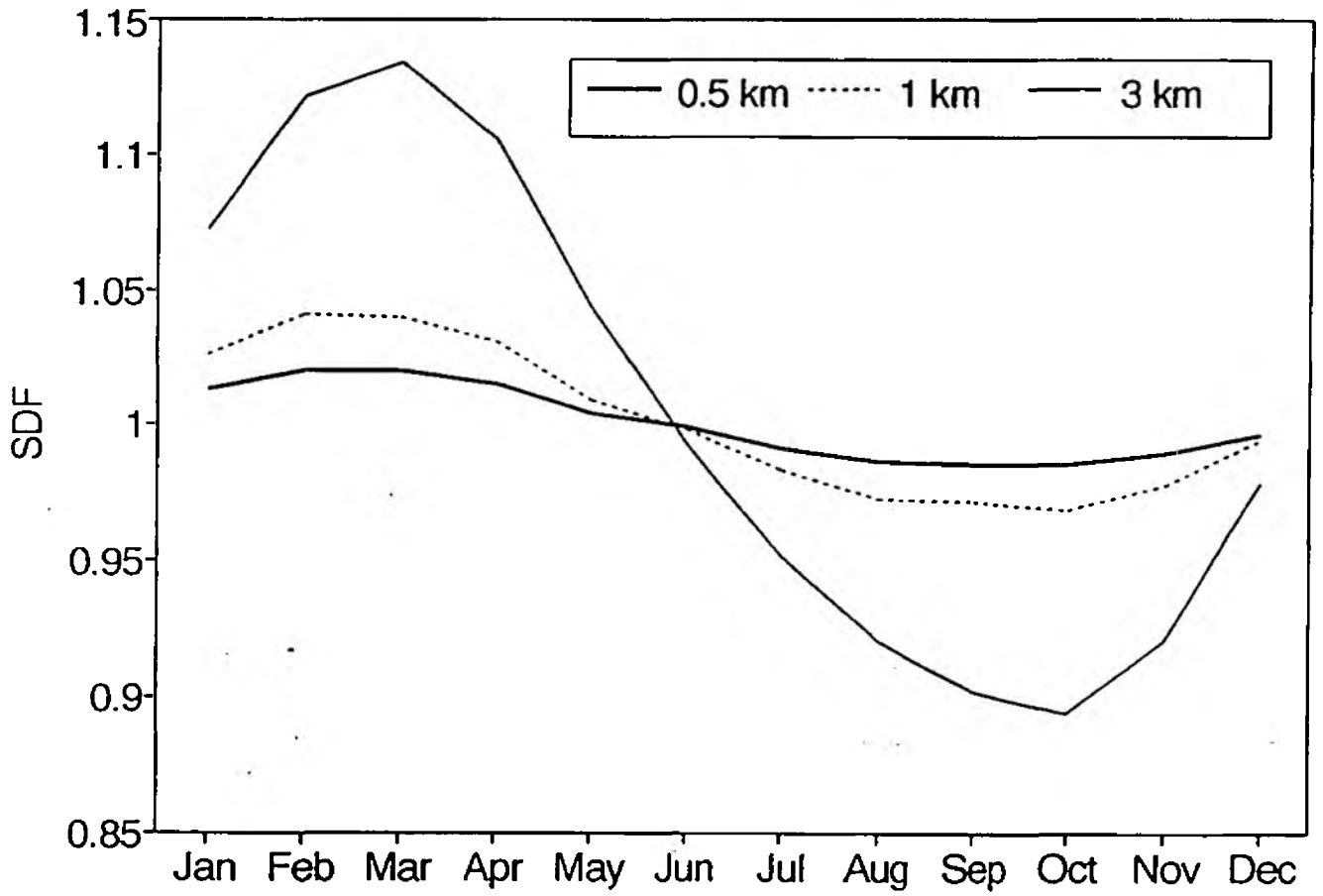

Fig 17. The mean monthly stream depletion factor (SDF) for different locations with constant abstractions.

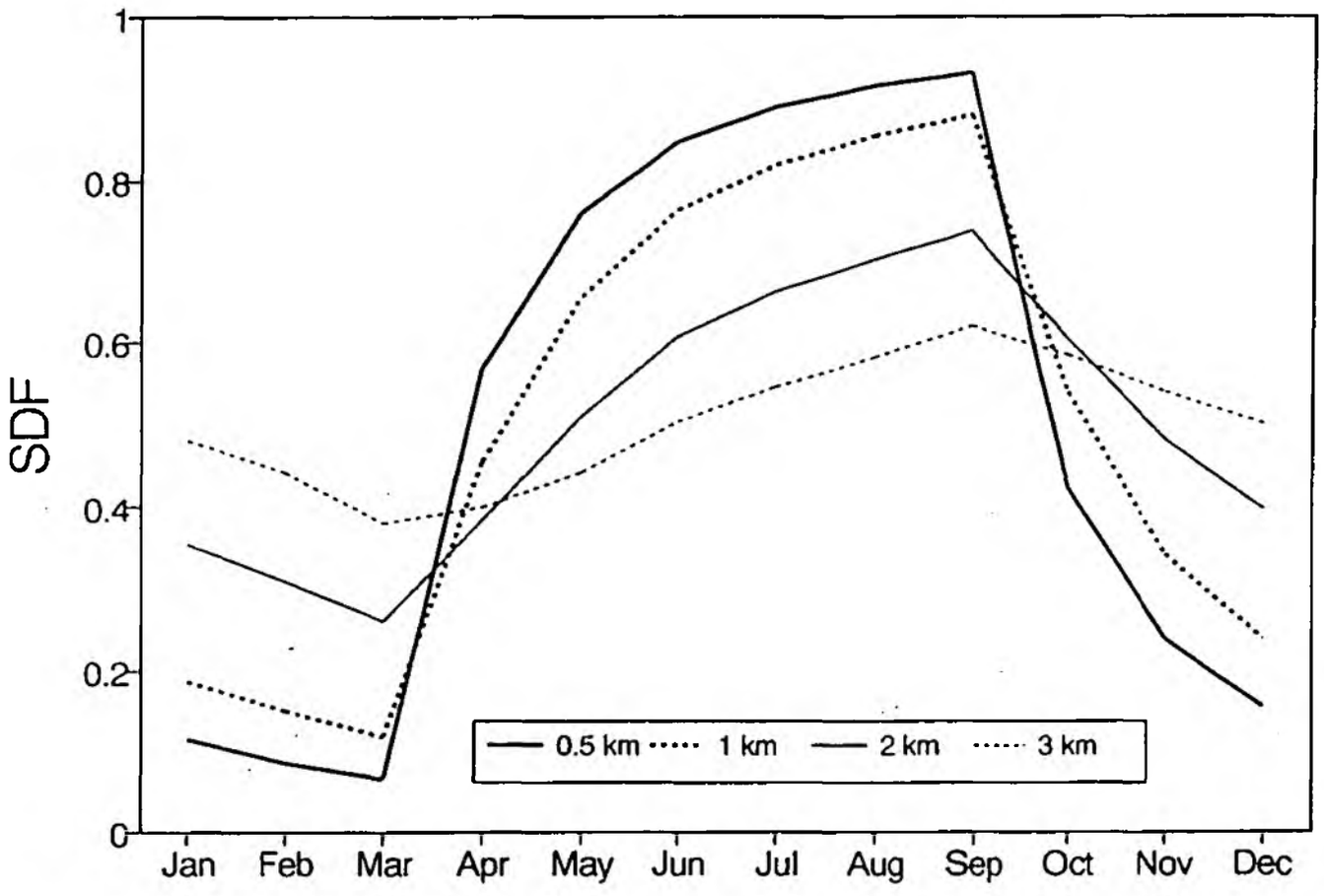

Fig 18. The mean monthly stream depletion factor (SDF) for different locations for six month (April-September) abstractions.

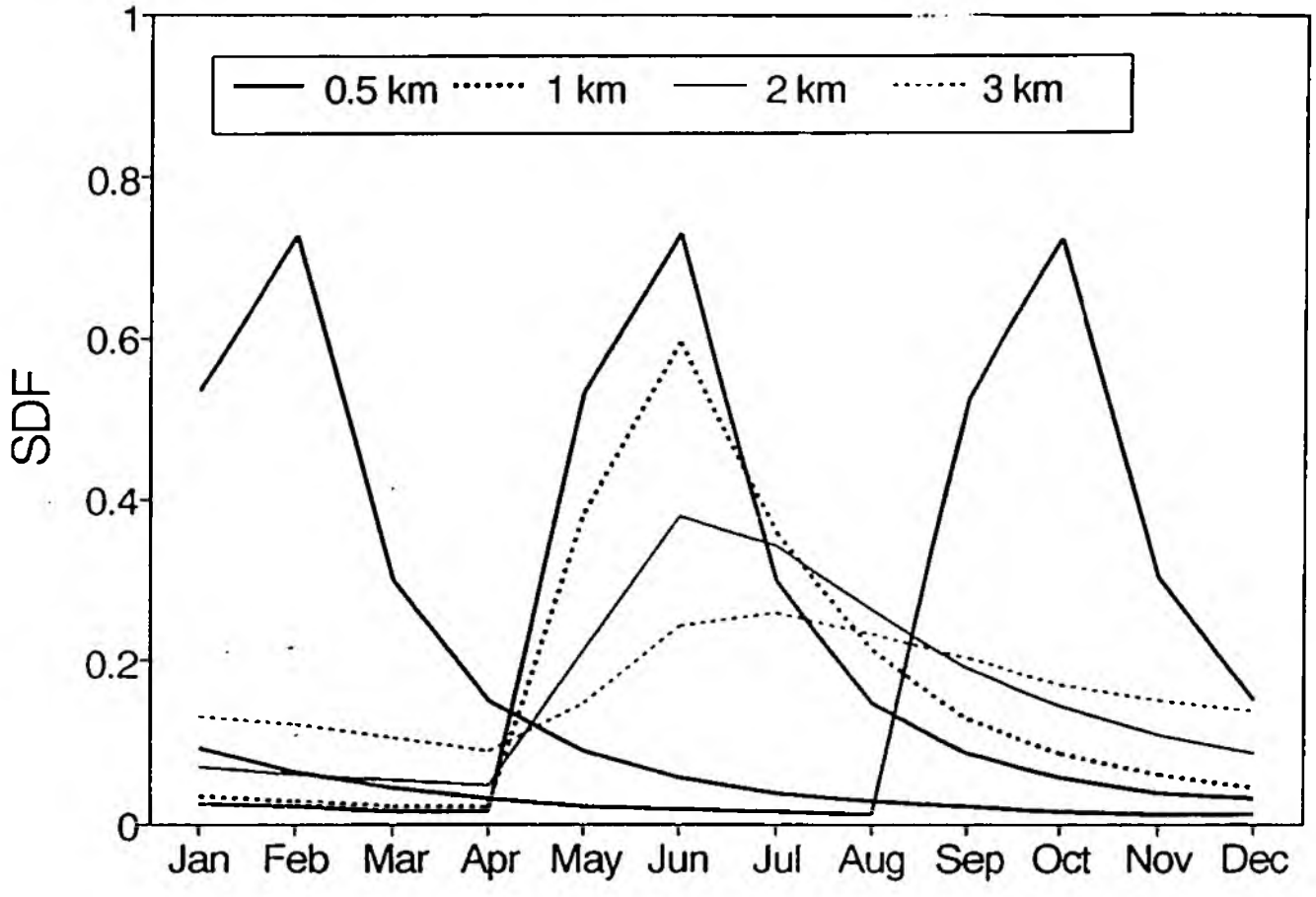

Fig 19. **The mean monthly stream depletion factor (SDF) for different locations for two month abstractions. The middle peak results from abstracting in May and June.**

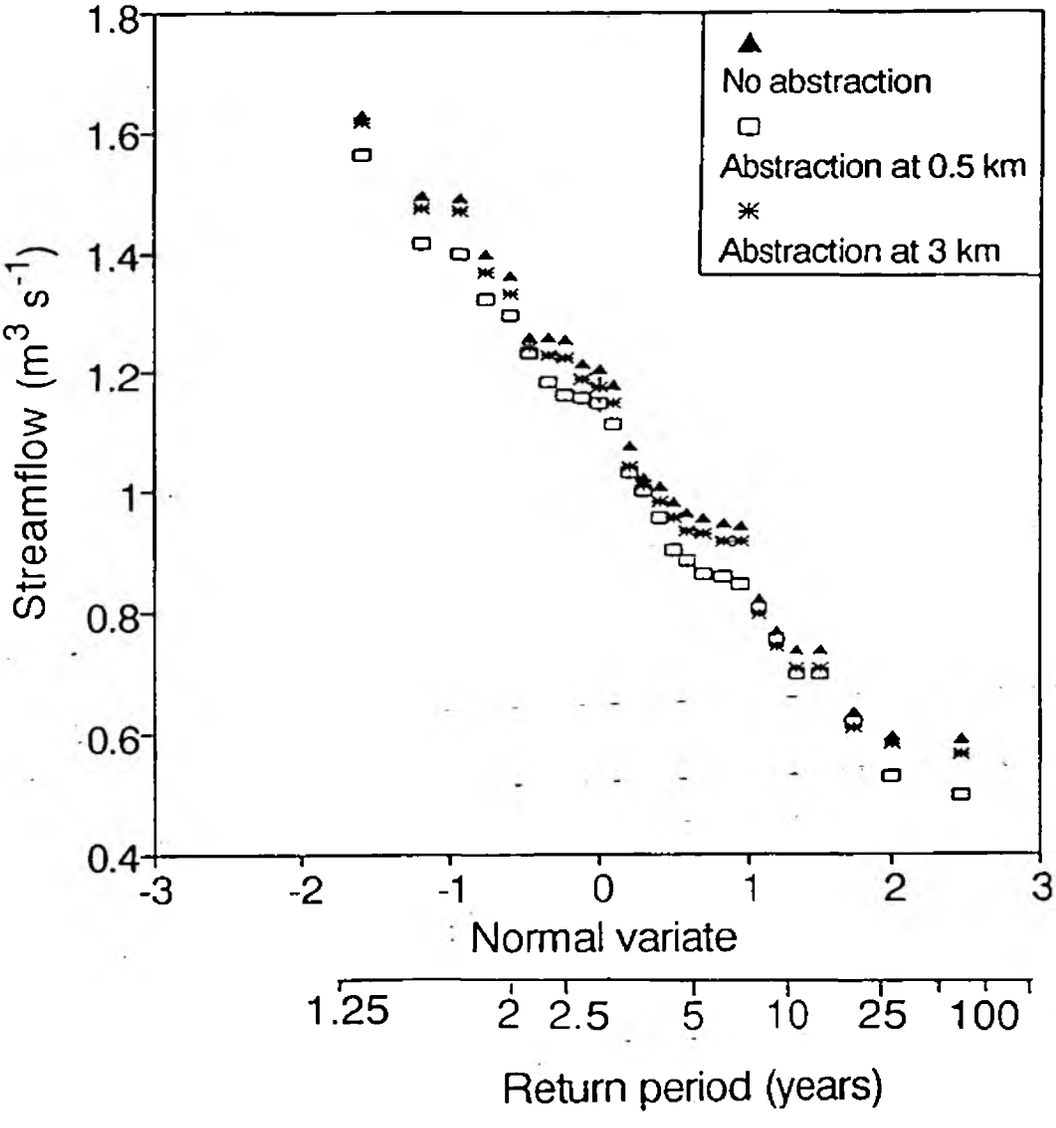

Fig 20. The effect of constant abstractions (500 $m^3 s^{-1}$) on the one month annual minima series.

Station name & number	Lambourn at Shaw 39019	Lambourn at Welford 39031	Lambourn at E.Sheff. 39032	Winterbourn at Bagnor 39033
Topographic catchment area (km^2)	234.1	176.0	154.0	49.2
Mean flow (m^3s^{-1})	1.72	1.02	0.77	0.17
Q95 (m^3s^{-1})	0.811	0.409	0.097	0.056
BFI	0.96	0.98	0.97	0.96

Table 1 Key variables for the four gauging stations in the Lambourn catchment.